<u>**Supporting information**</u>

Transmission electron microscopy of thiol-capped Au clusters on C: structure and electron irradiation effects

Lionel C Gontard[a,*] and Rafal E. Dunin-Borkowski[b]

[a] *Instituto de Ciencia de Materiales de Sevilla (CSIC), 41092, Sevilla, Spain*

[b] *Ernst Ruska-Centre for Microscopy and Spectroscopy with Electrons and Peter Grünberg Institute, Forschungszentrum Jülich, D-52425 Jülich, Germany*

* email: lionel.cervera@icmse.csic.es/lionelcg@gmail.com. Phone: +34 954489576

HRTEM imaging parameters

Electron-optical imaging parameters used for aberration-corrected HRTEM were measured using CEOS image corrector software. Representative values are given in Table S1. Multislice simulations of HRTEM images were performed in *JEMS* software using the optimized values shown in red in Table S1.

	Table S1	**Parameters used for image acquisition**					
	Conditions	Titan X-FEG, 1 s exposure, Ultrascan CCD, 2048 x 2048 pixels, 2x binning, 0.5 s readout time					
	Dose	2.9×10^6 e^-/nm^2 s, 1.97-µm-diameter illuminated area (46 A/cm^2)					
	Sample	Au@thiol on C film (300 kV)					
Aberrations		**C1 (Defocus, nm)**	**A1 (Two-fold Astigmatism, nm)**	**A2 (Three-fold Astigmatism, nm)**	**B2 (Coma, nm)**	**C3 (Spherical Aberration, µm)**	**A3 (Four-fold Astigmatism, µm)**
Measured with CEOS corrector	**Value**	-12.1	4.58	333.7	224.2	-4.5	2
	Angle	-	16.5˚	83˚	109.8˚	-	-160˚
Simulated*	**Value**	**13.4**	**5**	337.7	224.2	-4.5	-
	Angle	-	**16˚**	**224˚**	109.8˚	-	-
	* Defocus spread = 8 nm * Convergence semi-angle = 1 mrad						

Image contrast

Image contrast in experimental and simulated HRTEM images was calculated using the expression $\frac{I_{max}-I_{min}}{I_{max}+I_{min}}$ after normalization of the image intensity by that in vacuum.

Elastic energy transfer by high-energy electrons

The maximum energy transferred by a head-on elastic electron-atom collision was calculated using the equation

$$E_{max} = \frac{2147.66\, E_0\, (E_0+1.0220)}{A} \quad , \qquad [1]$$

where A is the atomic weight and E_0 is the kinetic energy of the incident electron expressed in MeV (Kandheval & Merzbacher, 1963). This expression assumes that an atom can be displaced if it receives an energy equal to or greater than a threshold energy (e.g., a binding energy or a displacement energy). Table S2 shows values of E_{max} calculated for three accelerating voltages for Au, C and S atoms.

Table S2	**Maximum kinetic energy transferred E_{max} (eV)**			
Accelerating voltage (kV)		**80**	**200**	**300**
Atom	**Au**	0.9	2.7	4.3
	C	15.8	43.7	70.9
	S	5.9	16.4	26.6

Binding, migration and displacement energies of Au and C

In addition to knock-on and sputtering, the energy transferred by an electron can break bonds, atoms can be evaporated from a cluster onto the support or they can migrate and form bonds at different sites. Table S3 provides a summary of calculated binding and migration energies of Au and C obtained from different references.

Table S3	Binding energy (eV)		Migration energy (eV)	
Au atom on graphene/graphite	0.45 0.35-0.37 0.6	(Jensen *et al.*, 2004) (1 layer) (Hardcastle *et al.*, 2013) (>3 layers) (Hardcastle *et al.*, 2013)	0.05-1 0.007 0.025	(Jensen *et al.*, 2004) (1 layer) (Hardcastle *et al.*, 2013) (>3 layers) (Hardcastle *et al.*, 2013)
Au atom at graphene edge	2 3-6.5	(Cretu *et al.*, 2010) (Wang *et al.*, 2012)	<1.5 2.2-2.5	(Wang *et al.*, 2012) (Gan *et al.*, 2008)
Au cluster on a-C	0.3/at	(Werner *et al.*, 2005)		
Au cluster (cohesive energy)	1.2/at (2at) ->2.8/at (20at) 3.8/at	 (Wang *et al.*, 2002) (Chan & *Yim*, 2013) bulk		
Au atom on Au(111) facet	3.4	(Mariscal *et al.*, 2010)		
C-C on graphene edge	<15	(Wang *et al.*, 2012, 2013)		
C-C in graphene	17	(Girit *et al.*, 2009)		
Au-Au displacement threshold	34	(Cretu *et al.*, 2012)		
C-C displacement threshold	17	(Cretu *et al.*, 2012)		
C sputtering	10	(Egerton *et al.*,2004)		

Binding energies of Au and S

Table S4 provides the binding energy of S-Au on a flat (111) surface and on Au adatoms.

Table S4	Binding energy (eV) at 300 K
S-Au (111)	1.84 (Mariscal *et al.*, 2010)
S-Au (adatom)	2.93 (Mariscal *et al.*, 2010)
Au cluster (cohesive energy)	1.2/at (2at) ->2.8/at (20at) (Wang *et al.*, 2002) (Chan & *Yim*, 2013) 3.8/at bulk
Au atom on Au(111) facet	3.4 (Mariscal *et al.*, 2010)

Sputtering rate of C film

In order to estimate the thickness of the a-C film, the electron-beam-induced sputtering rate at the exit surface of the specimen was estimated using the following procedure.

If high-angle elastic scattering occurs between the electrons and the sample, then displacement and sputtering effects are expected at the exit surface of the C film. Sputtering of surface atoms is most likely because they do not have to be accommodated in interstitial sites and are free to leave the specimen and to enter the vacuum of the microscope.

The sputtering rate *S* (in monolayers per second) is given by the equation

$$S = (J/e)(Z^2/AE_o)(1/E_s - 1/E_{max}) \cdot 3.54 \cdot 10^{-17} \qquad [2]$$

where (*J*/*e*) represents the incident current density in electrons/cm^2s, *A* is the atomic weight of C and E_s is the sputtering threshold energy (10 eV for C) (Egerton *et al.*, 2004). Fig. S1 shows the calculated sputtering rate for C plotted as a function of incident electron beam energy for an electron dose of $2.9x10^{20}$ electrons/cm^2s or 46 A/cm^2. The sputtering rate in nm/s is calculated by considering that one monolayer of C has a thickness of ~0.15 nm (approximately the length of a C-C bond). Hence, the curve represents 6.6 times *S*. Although the curve in Fig. S1 has not been corrected for relativistic effects, its maximum provides a good approximation for the sputtering rate, i.e, 0.09 nm/s at 300 kV (Egerton *et al.*, 2004). As we observed that holes form after approximately 3 minutes of observation, the estimated thickness of the film is 0.09 x 180 s =16 nm.

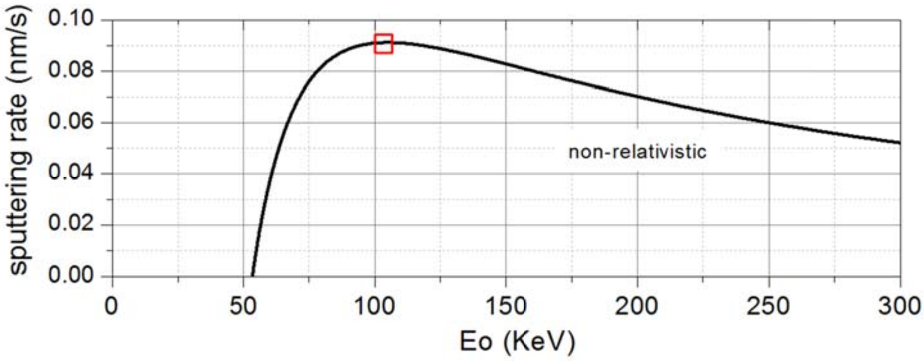

Fig. S1. Calculated sputtering rate of a-C plotted as a function of incident electron beam energy.

The inferred value of the specimen thickness is slightly higher than the nominal value of 10 nm given by the manufacturer of the TEM grid. A possible explanation is that the electron dose rate measured on the TEM phosphor screen is an underestimate of the true value, perhaps because the electron beam is convergent at the high magnification used in our experiments, resulting in a higher dose rate in the middle of the screen where the image is acquired.

References

Chan, K.T., Neaton, J.B., Cohen, M.L., 2008. First-principles study of metal adatom adsorption on graphene. *Phys. Rev. B* 77, 235430.

Chan, B., Yim W.-L., 2013. Accurate computation of cohesive energies for small to medium-sized gold clusters. *J. Chem. Theory Comput.* 9, 1964-1970.

Cretu, A.V., Krasheninnikov, J.A., Rodríguez-Manzo, J.A., Sun, L., Nieminen, R.M., Banhart, F., 2010. Migration and localization of metal atoms on strained graphene. *Phys. Rev. Lett.* 105, 196102.

Cretu, A.V., Rodríguez-Manzo, J.A., Demortière, A., Banhart, F., 2012. Electron beam-induced formation and displacement of metal clusters on graphene, carbon nanotubes and amorphous carbon. *Carbon* 50, 259-264.

Egerton, R.F., Li, P., Malac, M., 2004. Radiation damage in the TEM and SEM. *Micron* 35, 399-409.

Gan, Y., Sun, L., Banhart, F., 2008. One- and two-dimensional diffusion of metal atoms in graphene. *Small* 4, 587-591.

Girit, Ç.Ö., Meyer, J.C., Erni, R., Rossell, M.D., Kisielowski, C., Yang, L., Park, C.-H., Crommie, M.F., Cohen, M.L., Louie, S.G., Zettl, A., 2009. Graphene at the Edge: Stability and Dynamics. *Science* 323, 1705-1708.

Hardcastle, T.P., Seabourne, C.R., Zan, R., Brydson, R.M. D., Bangert, U., Ramasse, Q.M., Novoselov, K.S., Scott, A.J., 2013. Mobile metal adatoms on single layer, bilayer, and trilayer graphene: An ab initio DFT study with van derWaals corrections correlated with electron microscopy data. *Phys. Rev. B* 87, 195430.

Jensen, P., Blase, X., Ordejón, P., 2004. First principles study of gold adsorption and diffusion on graphite. *Surface Science* 564, 173-178.

Khandelwal, G.S., Merzbacher, E., 1963. Displacement cross sections for fast electrons incident on gold. *Phys. Rev.* 130, 1822-1825.

Mariscal, M.M., Olmos-Asar, J.A., Gutierrez-Wing, C., Mayoral, A., Yacamán, M.J., 2010. On the atomic structure of thiol-protected gold nanoparticles: a combined experimental and theoretical study. *Phys. Chem. Chem. Phys.* 12, 11785-11790.

Wang, J., Wang, G., Zhao, J., 2002. Density-functional study of Au_n(n=2-20) clusters: Lowest-energy structures and electronic properties. *Phys. Rev. B* 66, 035418.

Wang, H., Li, K., Cheng, Y., Wang, Q., Yao, Y., Schwingenschlögl, U., Zhang, X.X., Yang, W., 2012. Interaction between single gold atom and the graphene edge: A study via aberration-corrected transmission electron microscopy. *Nanoscale* 4, 2920-2925.

Wang, H., Feng, Q., Cheng, Y., Yao, Y., Wang,Q., Li, K., Schwingenschlögl, U., Zhang, X.X., Yang, W., 2013. Atomic bonding between metal and graphene. *J. Phys. Chem. C* 117, 4632-4638.

Werner, R., Wanner, M., Schneider, G., Gerthsen, D., 2005. Island formation and dynamics of gold clusters on amorphous carbon films. *Phys. Rev. B* 72, 045426.

Zan, R., Bangert, U., Ramasse, Q., Novoselov, K.S., 2012. Interaction of metals with suspended graphene observed by transmission electron microscopy. *J. Phys. Chem. Lett.* 3, 953-958.